Available online at www.sciencedirect.com
ScienceDirect
Procedia Engineering 121 (2015) 930 – 937
Procedia Engineering
www.elsevier.com/locate/procedia

9th International Symposium on Heating, Ventilation and Air Conditioning (ISHVAC) and the 3rd International Conference on Building Energy and Environment (COBEE)

Dynamic Performance of the Shading-Type Building-Integrated Photovoltaic Claddings

Liangliang Sun[a], Wenju Hu[b], Yanping Yuan[a,]*, Xiaoling Cao[a], Bo Lei[a]

[a] *School of Mechanical Engineering, Southwest Jiaotong University, Chengdu 610031, China*
[b] *Beijing Key Lab of Heating, Gas Supply, Ventilation and Air conditioning Engineering, Beijing University of Civil Engineering and Architecture, Beijing 100044 , China*

Abstract

Application of the shading-type Building-Integrated Photovoltaic (BIPV) claddings is one of the most effective approaches for reducing energy use in buildings and making buildings environment-friendly. PV modules are used as external shading devices and insulation panels as well. In this paper, the energy performance of the shading-type BIPV claddings is investigated under dynamic conditions. The design parameters of the shading-type BIPV claddings, including the tilt angles and azimuth angles of PV modules, the window to wall ratio of the building and the overhang length, are discussed based on the meteorological conditions of Hong Kong. Optimum designs of the shading-type BIPV claddings are reported for buildings with different orientations and window to wall ratios.

Peer-review under responsibility of the organizing committee of ISHVAC-COBEE 2015

Keywords: Shading-type building-integrated photovoltaic claddings; Optimum design; Energy saving; Dynamic performance

1. Introduction

Public awareness and the drastic increases in oil prices has encouraged many policy makers to promote renewable energy applications for reducing electricity consumption in buildings. The application of the Building-Integrated Photovoltaic (BIPV) technologies has become more widespread in the world. In fact, in a densely populated city like Hong Kong, integrating PV modules into buildings will be advantageous since no additional land is required for PV module installation, and better sunshine can be received on the facades of high-rise buildings. In order to efficiently use solar energy on the BIPV systems, a lot of studies [1-7] have been carried out for maximum energy benefits.

* Corresponding author. Tel.: +86-28-8763-4937; fax: +86-28-8763-4937.
E-mail address: ypyuan@home.swjtu.edu.cn

Peer-review under responsibility of the organizing committee of ISHVAC-COBEE 2015
doi:10.1016/j.proeng.2015.09.053

Nomenclature	
G	solar radiation
T	air temperature
t	time
ρ	density
C	specific capacity
l	thickness
h	heat transfer coefficient
λ	thermal conductivity
η	energy efficiency
H	height
P	length of overhang
R	window to wall ratio
β	Tilt angle

The shading-type BIPV claddings are installed on concrete walls or steal structure walls between windows. They can simultaneously generate electricity and provide shading for the windows and the concrete walls. Thus, the electricity saving produced by the shading-type BIPV claddings, including electricity generated by PV modules, electricity consumption reduction caused by the cooling load reduction of the window and the concrete wall, can then be evaluated, enabling the optimums design of the shading-type BIPV claddings to be obtained. The study presented in this paper aims to analyze the dynamic performance of the shading-type BIPV claddings and find out optimum designs for providing the most desirable energy saving effect in terms of electricity generation and electricity consumption reduction and to illustrate these results graphically for references for engineers or designers.

2. MATHMATICAL MODELS

2.1. The Dynamic Heat Transfer Model of Window

The transient heat transfer of the window can be analyzed by solving the heat conduction equation. As there is solar radiation passing through the glazing, in addition to conduction, the radiation absorbed along the glazing thickness should be included in the equation. The heat transfer balance equation is

$$\rho_g C_g l_g \frac{\partial T_g}{\partial t} = G_g + h_o\left(T_o - T_g\right) + h_{g-s}\left(T_s - T_g\right) + h_i\left(T_i - T_g\right) + \sum_{j=1}^{5} h_{g-j}\left(T_j - T_g\right) \quad (1)$$

where G_g is the total solar radiation absorbed by the window [8]. T_o and T_i are the outdoor air temperature and the indoor air temperature. ho and hi are the convective heat transfer coefficient of outside and inside surface of glazing. $h_{g\text{-}s}$ is the long wave radiant heat transfer coefficient between outside surface of glazing and the sky. $h_{g\text{-}j}$ is the long wave radiant heat transfer coefficient between the inside surface of glazing and the internal envelope.

2.2. The Dynamic Heat Transfer Model of Concrete wall

The concrete wall is modeled as a one dimensional slab of the finite thickness. It is assumed that the thermophysical properties of the concrete wall are homogeneous, isotropic and independent of the temperature. The transient heat transfer of the concrete wall can be expressed as follows

$$\left.\begin{aligned}
&\rho_w C_w \frac{\partial T_w}{\partial t} = \lambda_w \frac{\partial^2 T_w}{\partial x^2} \quad \left(0 < x < l_w\right) \\
&-\lambda_w \frac{\partial T_w}{\partial x}\Big|_{x=0} = h_o\left(T_o - T_w\right) + h_{w-s}\left(T_s - T_w\right) + G_w \\
&-\lambda_w \frac{\partial T_w}{\partial x}\Big|_{x=l_w} = h_i\left(T_i - T_w\right) + \sum_{j=1}^{5} h_{w-j}\left(T_j - T_w\right)
\end{aligned}\right\} \tag{2}$$

where G_w is solar radiation incident on concrete wall. $h_{w\text{-}s}$ is the long wave radiant heat transfer coefficient between outside surface of concrete wall and the sky. $h_{w\text{-}j}$ is the long wave radiant heat transfer coefficient between inside surface of concrete wall and internal envelope.

2.3. The Dynamic Heat Transfer Model of Photovoltaic module

If ρ_p, C_p and l_p is respectively the density, specific heat capacity and thickness of the PV cell, the heat transfer equation is expressed as

$$\rho_p C_p l_p \frac{\partial T_p}{\partial t} = (1-\eta)G_p + h_o\left(T_o - T_p\right) + h_{p-s}\left(T_s - T_p\right) + l_{fg}\frac{T_o - T_p}{\lambda_{fg}} + h_{w-p}\left(T_w - T_p\right) + h_o'\left(T_o - T_p\right) \tag{3}$$

where l_{fg} and λ_{fg} is the thickness and heat conductivity of the front glass of the PV module. G_p is the solar radiation absorbed by PV modules. η is the energy efficiency of PV cells [8].

3. SIMULATION PREREQUISITES

Fig. 1 shows the schematic of the exterior wall with the shading-type BIPV claddings. The ratio of the window height (H2) to the exterior wall height (3.2m) can be defined as the window to wall ratio (R). The window to wall ratios used in this study are 0.25, 0.50 and 0.75, respectively. When the overhang length (P) is chosen, different tilt angles are selected for different window to wall ratios to be sure that the value of H3 is no bigger than the value of H1. Table 1 shows the maximum tilt angles for different values of the overhang length.

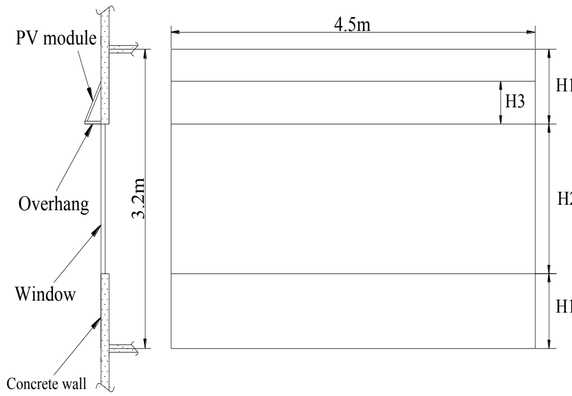

Fig. 1. The schematic of the shading-type BIPV claddings.

Table 1. Maximum tilt angles for different overhang lengths.

Overhang length (P)	Window to wall ratio (R)		
	0.25	0.5	0.75
0.1m	80°	80°	70°
0.2m	80°	70°	60°
0.3m	70°	60°	50°
0.4m	70°	60°	40°
0.5m	60°	50°	30°

4. RESULTS AND DISCUSSIONS

4.1. Electricity generation of PV modules

The annual electricity generation of PV modules is calculated when the reference energy efficiency of PV modules is set as 16%. Fig. 2. (a) shows the electricity generation per unit PV area. It indicates that the maximum point comes at the southwest-facing azimuth angle with a tilt angle of 20°. In general, PV modules produce more electricity annually at smaller tilt angles than they do at larger ones. The annual power output of PV modules decreases sharply when the tilt angles exceed 40°. If the south-facing PV modules have to be installed with a tilt angle of 80°, the annual power output is 106.8kWh/m^2, decreased by 27% compared with the largest value of 146.4kWh/m^2.

Fig. 2. (b) shows the total electricity generation produced by PV modules when the window to wall ratio is 0.25 and PV modules are arranged south-facing. It indicates that the total power output of PV modules increases when the tilt angle and the overhang length increase. The maximum electricity generation is 598.26kWh when the tilt angle of PV modules equals 70° and the length of the overhang equals 0.4m.

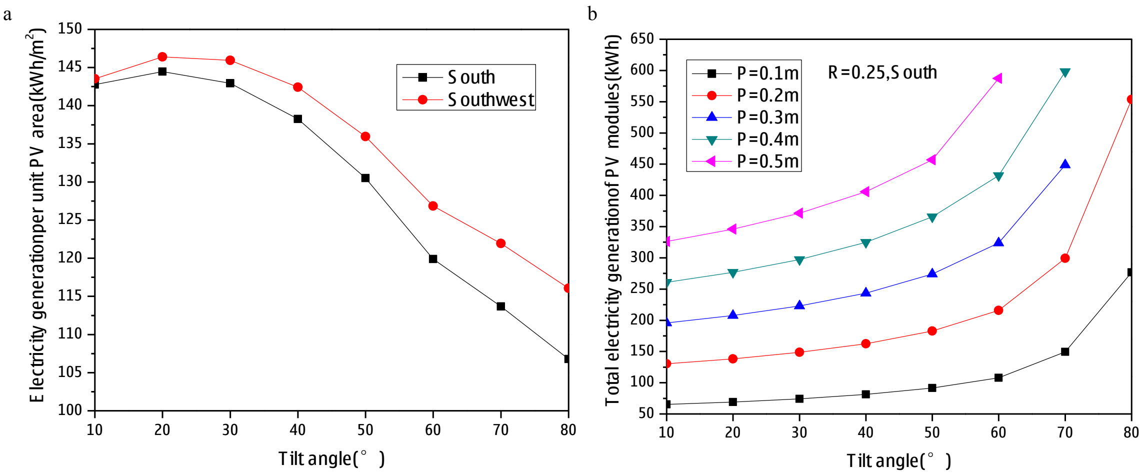

Fig. 2. (a) Electricity generation per unit PV area; (b) Total electricity generation of PV modules.

4.2. Cooling load reduction of window

The cooling load reduction ratio is shown in Fig. 3. (a). It can be observed that the shading effect of the shading-type BIPV claddings on the south-facing window is more significant than that on the southwest-facing window. For the same orientation and the same overhang length, the cooling load reduction ratio decreases as the window to wall ratio increases. The cooling load reduction ratio of the south-facing window is as large as 58.5% when the window to wall ratio equals 0.25 and the overhang length equals 0.5m. While the overhang length is 0.10m, the cooling load reduction ratio is only 5% for the window to wall ratio of 0.75. Fig. 3. (b) shows the annual total cooling load reduction of the window. It indicates that the window of larger window to wall ratio can obtain more cooling load reduction. The total cooling load reduction of south-facing window is smaller that of southwest-facing window because the southwest-facing window can produce more cooling load than that of south-facing window.

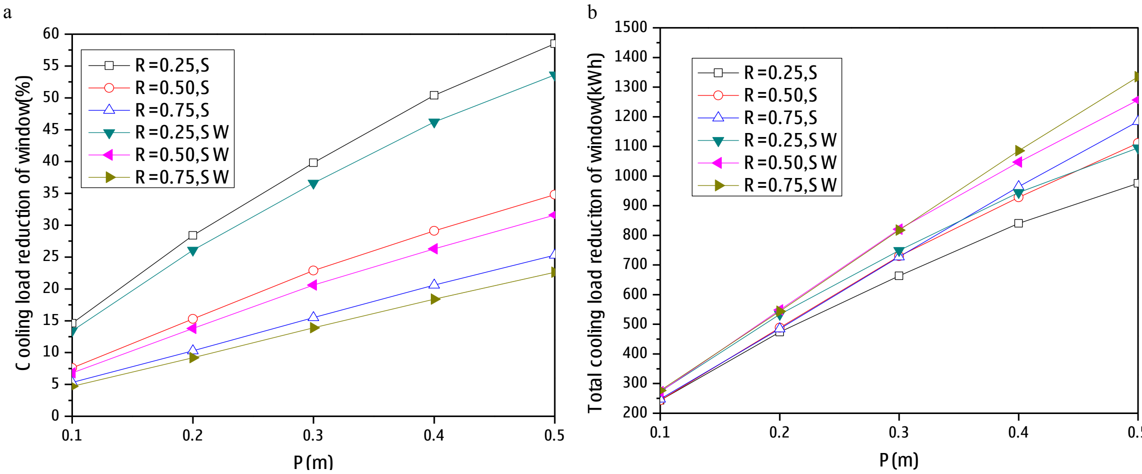

Fig. 3. (a) Cooling load reduction per unit window; (b) Total cooling load reduction of the window.

4.3. Cooling load reduction of concrete wall

The cooling load reduction ratio of concrete wall with the overhang length of 0.3m and the tilt angle of 20° is shown in Fig. 4. For the same window to wall ratio, concrete wall facing southwest has larger cooling load reduction ratio than that facing south. As the overhang length and the window to wall ratio increases, the cooling load reduction ratio decreases for both the southwest-facing and south-facing concrete wall. When the tilt angle increases, the cooling load reduction ratio firstly decreases and then increases. It can be concluded that if concrete wall gains enough radiant heat from PV modules, the cooling load reduction can be negative.

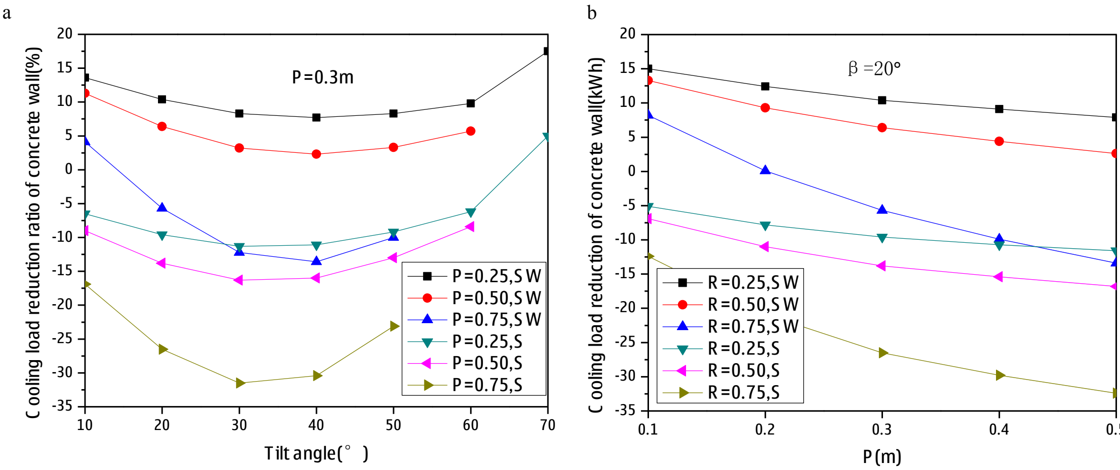

Fig. 4. Cooling load reduction of concrete wall (a) P=0.3m; (b) β=20°.

4.4. Total electricity saving of the shading-type BIPV claddings

As mentioned above, the electricity generation of PV modules and the cooling load reduction of the exterior wall produced by the shading-type BIPV claddings will simultaneously contribute to total electricity saving in buildings. It is necessary to analyze the combined effects of these two contributions and to evaluate the optimum position of the shading-type BIPV claddings so that maximum electricity saving is achieved. By using the COP of the HVAC system, the annual cooling load reduction can be converted into annual electricity consumption reduction. Supposing that the building is cooled by an air cooled HVAC system, the value of COP is set to be 2.8 [9].

Fig. 5-7 indicate that the reduction ratio increases with the tilt angle and the overhang length increases. The reduction ratio of the south-facing exterior wall is larger than that of the southwest-facing exterior wall when the overhang length, the tilt angle and the window to wall ratio is the same. For the same tilt angle and the same overhang length, the reduction ratio decrease as the window to wall ratio increases. The maximum reduction ratio of 96.1% occurs when PV modules have the surface azimuth angle of 0°, the tilt angle of 70° and the overhang length of 0.4m. The southwest-facing PV modules with the tilt angle of 10° and the overhang length of 0.1m can only produce the reduction ratio of 4%. Table 2 summarizes the optimum designs for different surface azimuth angles and window to wall ratios.

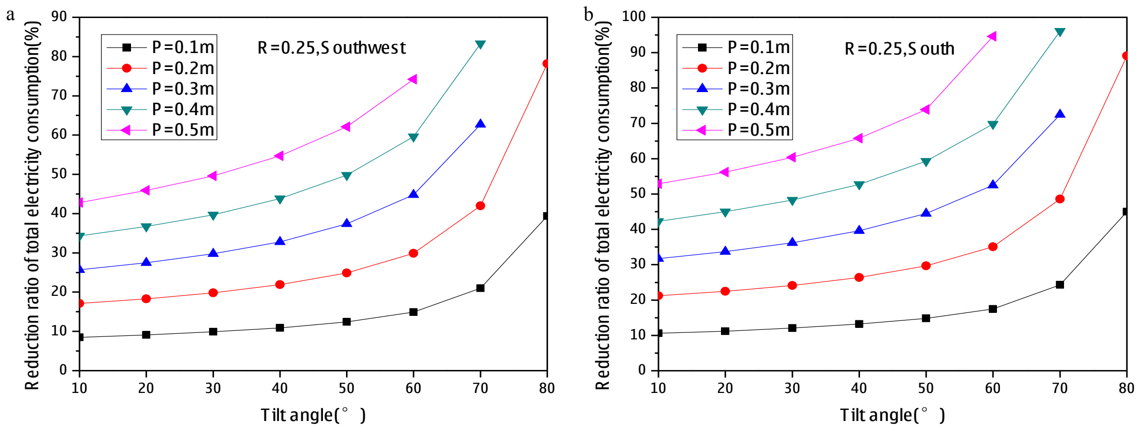

Fig. 5. Reduction ratio of total electricity consumption of R=0.25 (a) southwest; (b) south.

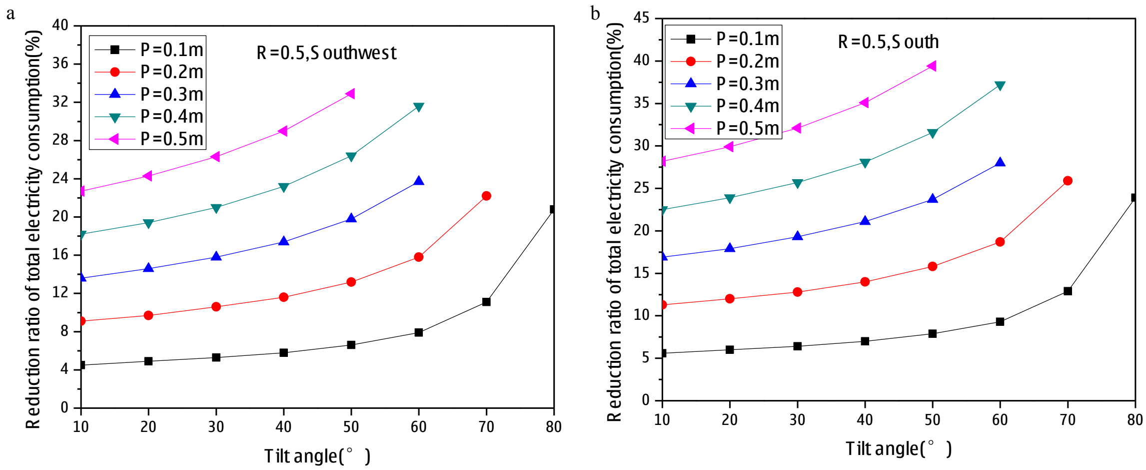

Fig. 6. Reduction ratio of total electricity consumption of R=0.5 (a) southwest; (b) south.

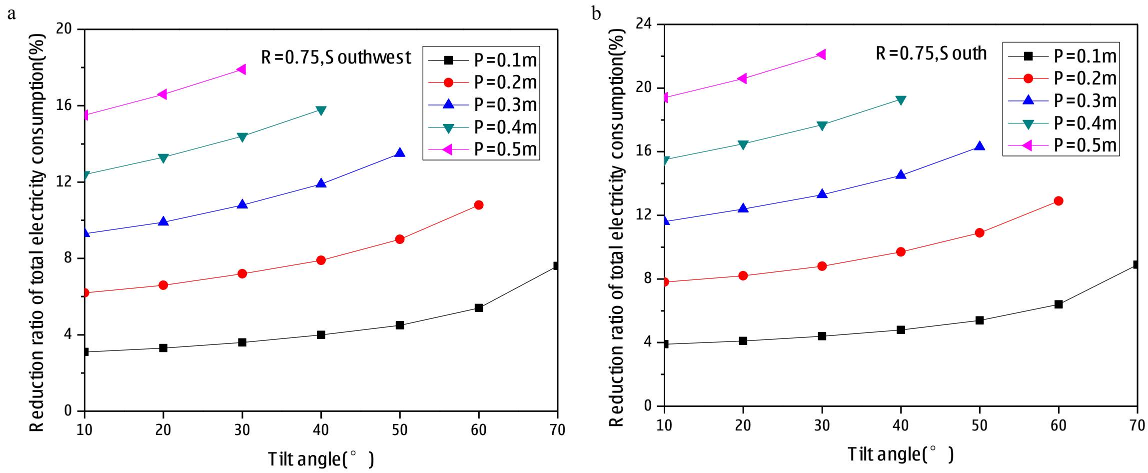

Fig. 7. Reduction ratio of total electricity consumption of R=0.75 (a) southwest; (b) south.

Table 2. Optimum designs of PV modules and reduction ratio of electricity consumption.

	Overhang length (P)	Tilt angle (β)	Reduction ratio
R=0.25,SW	0.4m	70°	83.3%
R=0.25,S	0.4m	70°	96.1%
R=0.50,SW	0.5m	50°	32.9%
R=0.50,S	0.5m	50°	39.4%
R=0.75,SW	0.5m	30°	17.9%
R=0.75,S	0.5m	30°	22.1%

As shown in Fig. 8, when the window to wall ratio is small, the power generated by PV modules dominates the total electricity savings. However, as the window to wall ratio increases, the electricity saving due to window cooling load reduction becomes significant on the total electricity saving. The electricity saving produces by concrete wall just takes a very little portion of the total electricity saving, just within 1%. In addition, when the window to wall ratio is large, the contribution of concrete wall to the total electricity saving is negative.

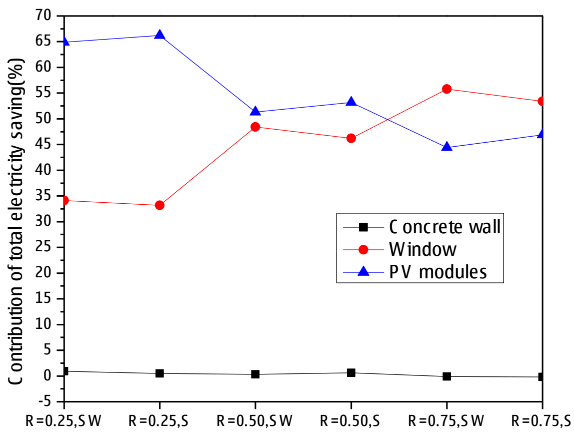

Fig. 8. Contribution of total electricity saving.

5. CONCLUSIONS

The impact of tilt angles, surface azimuth angles, overhang lengths and window to wall ratios on the energy performance of the shading-type BIPV claddings has been analyzed in this paper, in terms of annual electricity generation of PV modules and electricity reduction due to cooling load reduction of windows and concrete walls. For the power output of PV modules, the shading-type BIPV claddings installed on the southwest façade can produce more electricity per unit PV area annually at the tilt angle of 20°.

Different optimum tilt angles of the shading-type BIPV claddings are obtained for different surface azimuth angles and window to wall ratios to achieve the maximum electricity saving. With the same wall to window ratio and overhang length, PV modules can produce more electricity saving at large tilt angles than those of small tilt angles. Electricity generation due to PV modules and electricity consumption reduction due to window contribute a great majority of total electricity saving, and the electricity saving due to concrete wall can be ignored specially for buildings with large window to wall ratio. These simulation results are good references for engineers or designers to integrate the shading-type BIPV claddings on building facades.

Acknowledgements

The work described in this paper was supported by Beijing Key Lab of Heating, Gas Supply, Ventilating and Air Conditioning Engineering (Project No. NR2013K08), Sichuan Province Youth Science and Technology Innovation Team of Building Environment and Energy Efficiency (Project No. 2015TD0015) and the Fundamental Research Funds for the Central Universities (Project No. 2682015CX038).

References

[1] T.T. Chow, K.F. Fong, W. He, Z. Lin, A.L.S Chan, Performance evaluation of a PV ventilated window applying to office building of Hong Kong, Energ. Buildings. 39 (2007) 643-650.
[2] T.T. Chow, K.F. Fong, G. Pei, J. Ji, W. He, Potential use of photovoltaic-integrated solar heat pump system in Hong Kong, Appl. Therm. Eng. 30 (2010) 1055-1072.
[3] T.Y.Y. Fung, H.X. Yang, Study on thermal performance of semi-transparent building-integrated photovoltaic glazings, Energ. Buildings. 40(3) (2008) 341-350.
[4] J. Ji, W. He, H.N. Lam, The annual analysis of the power output and heat gain of a PV-wall with different integration mode in Hong Kong, Sol. Energ. Mat. Sol. C. 71 (2002) 435-448.
[5] J. Ji, T.T. Chow, W. He, Dynamic performance of hybrid photovoltaic/thermal collector wall in Hong Kong, Appl. Energy. 83 (2003) 42-54.
[6] L. Lu, H.X. Yang, A Study on Simulations of the Power Output and Practical Models for Building Integrated Photovoltaic Systems, J. Sol. Energ. Eng. 126 (2004) 929-935.
[7] H.X. Yang, L. Lu, The Optimum Tilt Angles and Orientations of PV Claddings for Building-Integrated Photovoltaic (BIPV) Applications, J. Sol. Energ. Eng. 129 (2007) 253-255.
[8] H.A. Zondag, D.W. DE Vries, W.G.J. VAN Helden, R.J.C. VAN Zolingen, The Thermal and Electrical Yield of A PV-Thermal Collector, Sol. Energy. 72 (2002) 113-128.
[9] F.W.H. Yik, J. Burnett, I. Prescott, Predicting Air-Conditioning Energy Consumption of A Group of Buildings Using Different Heat Rejection Methods, Energ. Buildings. 33 (2001) 151-166.